

MEMORANDUM

To: Dan Fabricant

From: Warren Brown

Date: 23 May 2002

Subject: Binospec Thermal Analysis V: Deflections due to Temperature Changes

1. INTRODUCTION

This is the fifth in a series of memos concluding the Binospec thermal analysis. This memo estimates angular deflections caused by temperature differences in the spectrograph.

I begin by introducing spherical bending calculations. I then present the sensitivities of the optics, so that shifts on the Binospec image plane can be estimated from deflections. I focus on the deflection of the Binospec optical bench, but I also estimate deflections for other parts of the Binospec system. A finite element model created by Henry Bergner is used to study the optical bench deflections in detail.

2. SPHERICAL BENDING

The spherical bending deflections calculated in this memo are for the case of a uniform temperature difference between the top and bottom of an unconstrained circular disk. This case is useful because it can be solved analytically. The disk geometry is also a good match to the Binospec optical bench. I extend the spherical bending calculations to temperature differences across other disk-like components (the lenses, the camera base, and the fold mirror structure), though these latter calculations are estimates at best.

What we are truly interested in is the *rate* at which objects tilt. To estimate rates, I divide the deflection by the time scale of a temperature difference. The times and magnitudes of the temperature differences come from the baseline Binospec model described in the “Baseline Model Result” memo.

I used Roark and Young’s *Formulas for Stress and Strain* to make the calculations, but I found that their complicated formulas reduce to the simple case of spherical bending. Thus I use the following spherical bending relations from Dan Fabricant’s July, 22, 1994 “Optical Table for the Hectospec Spectrograph” memo.

The deflection caused by spherical bending is related to the radius of curvature. The radius of curvature R of a sphere can be derived from

$$\frac{R+t}{R} = r + \varepsilon r, \tag{1}$$

where r is the radius of the disk, t is the thickness of the disk, and ε is the change in radius ($r\gamma\Delta T$). The coefficient of thermal expansion γ is assumed to be uniform throughout the disk. Solving for the radius of curvature R , we have

$$R = \frac{t}{\gamma\Delta T} \tag{2}$$

The equation for the sag of a sphere is

$$z = \frac{r^2/R}{1 + \sqrt{1 - (r/R)^2}}. \quad (3)$$

The slope of the sphere is

$$\frac{dz}{dr} = \frac{r/R}{\sqrt{1 - (r/R)^2}}. \quad (4)$$

I note that the slope is approximately linear with r , since $(r/R)^2$ is very small for our cases of interest. Finally, the deflection angle θ is

$$\theta = \arctan\left(\frac{dz}{dr}\right). \quad (5)$$

3. SENSITIVITIES

The deflections calculated from Equation 5 are meaningful only if we know how they affect the optical performance of Binospec. Dan Fabricant's Binospec optical sensitivity analysis is found in the instrument database, document #295.

The optical sensitivity document is a little confusing, so let me briefly explain it here. x , y , and z are local coordinates at each surface, with z always increasing in the direction of the optical axis. Each optical surface is adjusted with an arbitrary shift of 0.010 inches and a rotation of 3 arcminutes around the three coordinate axes. For each adjustment, Zemax calculates the resulting shifts dx and dy (in μm) on the image plane, the shift dz (in μm) in focus, and the resulting RMS spot size (in μm). The CCD has 13.5 μm pixels, and the whole Binospec error budget is 1-2 pixels. I re-calculate the sensitivities in Dan's analysis to allow a direct comparison with the deflections calculated in later sections.

Table 1 lists the *value* of the shift or rotation that will *produce* a 1 pixel (13.5 μm) shift on the image plane. Δx and Δy are the de-centers (in thousandths of an inch) of the lens which will produce a 1 pixel x and y shift, respectively, on the image plane. Δz is the shift along the optical axis that will produce a +13.5 μm z focus shift. ϕ_x and ϕ_y are rotations about the x and y axes that will produce 1 pixel y and x shifts, respectively, on the image plane. Note that large values in Table 1 are good; large values mean an optical element requires a lot of movement to produce a 1 pixel shift on the CCD.

The grating is the optical element most sensitive to deflections: a 4 arcsec tilt of the grating will cause a 1 pixel shift on the image plane. Lens group air-glass surfaces and the collimator fold mirror are also sensitive to deflections.

The lens groups as a whole are rather insensitive to deflections. The appropriate way to sum the sensitivity for a lens group is

$$\frac{1}{\phi_{tot}} = \sum_i \frac{1}{\phi_i}. \quad (6)$$

Sums of the deflections in a lens group show that many of the image shifts cancel out: for example, camera lens group 3 has an $-1/14 + 1/14 \Rightarrow \infty$ angle to cause a 1 pixel image shift. In reality, tilting a whole lens group involves both tilts and offsets, thus the simple lens group sum in Eqn. 6 underestimates the true lens group sensitivity.

TABLE 1
 BINOSPEC SENSITIVITIES
 Shifts and Rotations that produce 1 pixel shifts on the CCD

Element	Δx (mil)	Δy (mil)	Δz (mil)	ϕ_x (arcsec)	ϕ_y (arcsec)
FOLD MIRROR ASSEMBLY					
Center Fold	∞	∞	-3	34	-29
Side Fold	∞	∞	3	-19	14
COLLIMATOR Lens Group 1					
BAL15YP	3	3	-5	-26	29
SFSL5Y	6	6	-41	25	-27
COLLIMATOR Lens Group 2					
PBM2Y	1	1	7	-24	26
PBL6Y	-8	-7	-18	12000	-24000
BAL35Y	1.5	1.4	35	-1500	1700
CAF2	-4	-4	-6	3000	-3000
PBL6Y	-1	-1	2	29	-31
FOLD MIRROR	∞	∞	-1	5	-8
COLLIMATOR Lens Group 3					
BSM51Y	-2	-2	-2	16	-17
CAF2	1	1	1	-13	14
GRATING					
	∞	∞	∞	4	4
CAMERA Lens Group 1					
BAL35Y	2	2	13	-14	14
CAF2	-10	-11	-270	14	-14
CAMERA Lens Group 2					
CAF2	1	1	3	-15	15
BAL35Y	-5	-5	-7	-2400	2000
CAF2	-7	-7	-13	1700	-1900
PBM2Y	1	1	1	19	-19
CAMERA Lens Group 3					
FPL51Y	1	1	2	-24	24
NACL	-9	-9	-6	-3000	2700
CAF2	-10	-10	2	40	-40
DEWAR WINDOW					
BSM51Y	-8	-8	-4	-600	600

4. OPTICAL BENCH

4.1. Spherical Bending Calculations

Temperature differences arise across the optical bench because the optical bench divides Binospec in half. We perform the spherical bending calculation for the top-to-bottom axial temperature differences that result from “typical” ($\pm 3^\circ$ C variations over 24 hours) and “extreme” ($\pm 10^\circ$ C variations over 8 hours) MMT dome temperatures. Table 2 summarizes the worst-case deflections θ and displacements z at the edge of the $r = 1.07$ m optical bench, and an estimate of the image shift on the CCD. I use times from the baseline Binospec model to estimate the rates.

The rate of deflection $d\theta/dt$ at the edge of the optical bench is 0.25 arcsec per hour for the baseline Binospec model operating in “typical” MMT temperatures. The rate of deflection of the optical bench is four times worse – 1 arcsec per hour – for a Binospec without an entrance window and operating in “extreme” MMT temperatures.

TABLE 2
OPTICAL BENCH
Spherical Bending — Axial Temperature Gradient

Case	ΔT ($^\circ$ C)	$\Delta T/dt$ ($^\circ$ C/hr)	θ_{worst} (arcsec)	$d\theta/dt$ (arcsec/hr)	z_{worst} (mil)	dz/dt (mil/hr)	shift (pix)	shift/dt (pix/hr)
Typical	± 0.075	0.006	2.5	0.25	0.25	0.025	0.4	0.04
Extreme	± 0.15	0.03	5.0	1.0	0.5	0.1	0.8	0.17

The grating and camera optics sit at $r \sim 0.7$ m and so will experience $\sim 2/3$ the value of the deflection in Table 2, or $\theta = 1.6$ arcsec. Table 1 shows that this deflection at the grating will shift the image on the CCD by $1.6/4 = 0.40$ pixels. By comparison, the camera lens groups shift the image on the CCD by less than 0.05 pixel (because the deflections in the lenses largely cancel out).

The typical *rate* of deflection at the grating will cause a $0.16/4 = 0.04$ pixel/hr image shift on the CCD. This is well within the Binospec error budget. “Extreme” temperatures will cause a 4 times greater shift of 0.17 pixel/hr at the grating. This worst case is within the Binospec error budget but more worrisome. Clearly, a well-insulated Binospec reduces the rate of thermal deflection of the optics.

4.2. Finite Element Model

Temperature differences other than the axial case will occur in the Binospec optical bench: radial center-to-edge differences from the insulation, local hot spots from stepper motors, and perhaps diametral edge-to-edge differences caused by the orientation of the spectrograph. To better study these temperature differences we turn to a finite element model created by Henry Bergner.

Henry’s finite element model has 5 layers for the optical bench core and a layer for the top and bottom face sheets. Each element has approximate area 1 in². The finite element model results for unit temperature differences for four cases are plotted in Figures 1 - 4. The plots show the

deflection “y rotation” as a function of radius, above which I sketch the shape of the optical bench deformation. The unit temperature differences are identical, within a factor of 2, of the temperature differences from the baseline Binospec model.

I summarize the worst-case deflections, displacements, and image shifts in Table 3. The worst-case deflections are right next to the hot spot or at the edge of the optical bench (for radial and diametral temperature gradients). I use times from the baseline Binospec model to estimate bending rates.

TABLE 3
OPTICAL BENCH
Finite Element Model — Unit Temperature Gradients

Case	ΔT (° C)	$\Delta T/dt$ (° C/hr)	θ_{worst} (arcsec)	$d\theta/dt$ (arcsec/hr)	z_{worst} (mil)	dz/dt (mil/hr)	shift (pix)	shift/dt (pix/hr)
Axial	0.1	0.01	3.5	0.35	0.35	0.035	0.60	0.060
Radial	1	0.1	1.0	0.1	0.06	0.006	0.17	0.017
Diametral	1	0.1	0.4	0.04	0.06	0.006	0.07	0.007
Hot Spot	0.1	0.07	0.2	0.13	0.005	0.003	0.05	0.033

Figure 1 plots the deflection for a 1° C **axial** top-to-bottom temperature difference. When scaled for a 0.1° C axial temperature difference, the maximum deflection at the edge of the optical bench is 3.5 arcsec. *This deflection agrees to 10% with the simple spherical bending calculation value for $\Delta T = 0.1^\circ$.* The rate of deflection at the grating (for a 0.1° temperature difference) will cause a 0.06 pixel/hr image shift on the CCD.

Figure 2 plots the deflection for a 1.07° C **radial** center-to-edge temperature difference. 1.07° C is the maximum radial temperature difference along the optical bench in the baseline Binospec model (using “extreme” MMT temperatures). The deflection at the edge of the optical bench varies between -0.6 arcsec and +1 arcsec. This turn-over at the edge of the optical bench is real, caused by the bowing of the core. The rate of deflection at the grating will cause a 0.02 pixel/hr image shift on the CCD.

Figure 3 plots the deflection for a 1° C **diametral** edge-to-edge temperature difference. The deflection along the optical bench is constant at -0.4 arcsec and then flares at the edge to +0.2 arcsec. The rate of deflection at the grating will cause a 0.007 pixel/hr image shift on the CCD.

Figure 4 plots the deflection for a 0.1° C **hot spot** at the center of the optical bench. 0.1° C comes from operating the filter changer motor for 1.5 hours in imaging mode, which is equivalent to an average heat input of 0.5 Watts over 1.5 hours. The deflection peaks at 0.2 arcsec. The rate of deflection, if the hot spot were located next to the grating turret, would cause a 0.033 pixel/hr image shift on the CCD.

Note that a hot spot at the grating may cause an image shift nearly as large as the image shift due to the optical bench axial temperature difference. This suggests that no motor should be directly mounted to the optical bench except by a thermal stand-off (i.e. a delrin or nylon pad). Image shifts due to reasonable radial and diametral temperature differences along the optical bench are 3 - 8 times smaller than image shifts caused by the axial case.

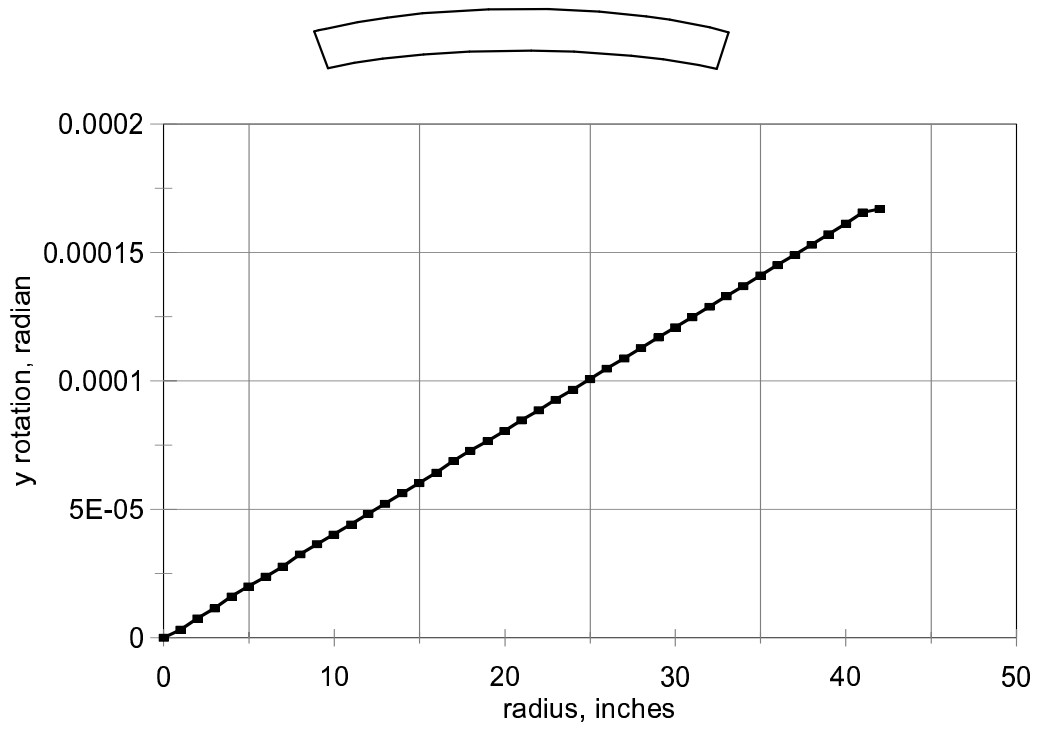


Fig. 1.— Tilt for a 1° C **axial** top-to-bottom temperature difference.

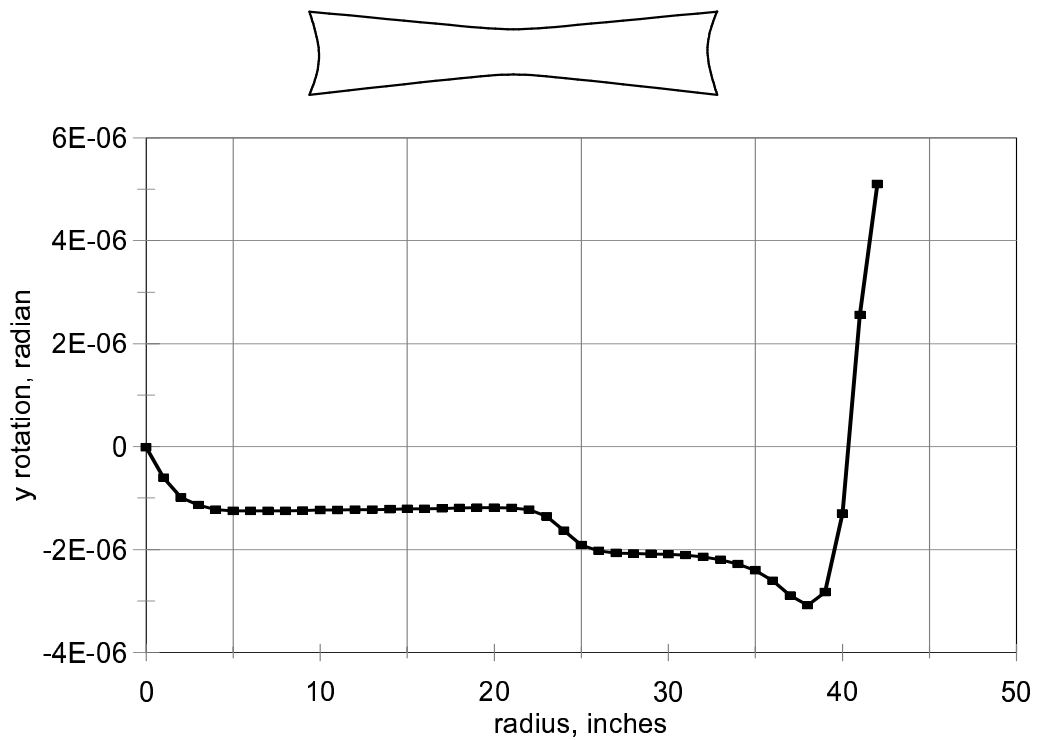


Fig. 2.— Tilt for a 1.07° C **radial** center-to-edge temperature difference.

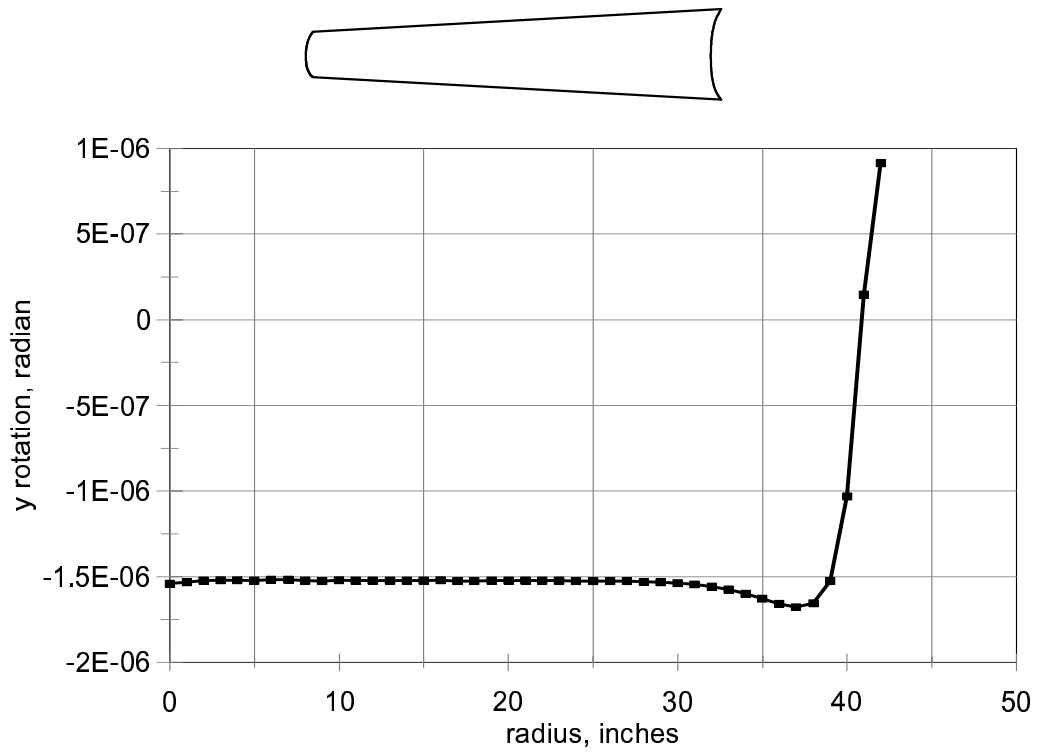


Fig. 3.— Tilt for a 1° C **diametral** edge-to-edge temperature difference.

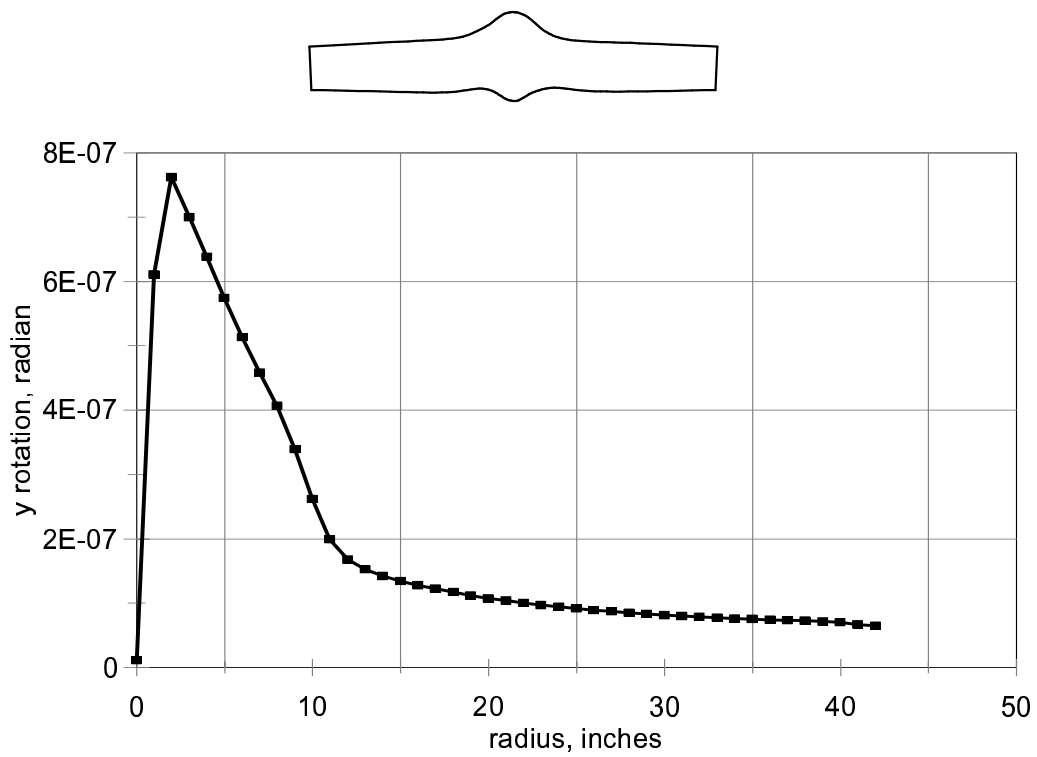


Fig. 4.— Tilt for a 0.1° C **hot spot** at the center of the optical bench.

5. OTHER BINOSPEC COMPONENTS

5.1. Lens Deflections

I perform deflection calculations on Binospec lenses well matched by the glass disk geometry. For a unit 1° C axial temperature difference along a lens, edge deflections are 3-10 arcsec and displacements are 0.4 - 1.2 mil. These values are at the level of the spherical bending tolerances taken from Dan Fabricant's optical sensitivity memo.

The worst axial temperature difference actually seen in the baseline Binospec model is a $\sim 0.1^\circ$ C drop across collimator lens group 1 and camera lens group 3 (a high conductivity CaF_2 lens plus two other, low conductivity lenses). Thus axial temperature differences should not cause significant disk deflection in the Binospec lenses.

5.2. Camera Base and Fold Mirror Structure

The fold mirror structure and the camera base are relatively flat pieces with temperature differences across them. Thus I use Equation 5 to estimate deflections. I use temperature differences from the baseline Binospec model for "typical" MMT temperatures. Table 4 summarizes the worst-case deflections and displacements.

The rates of deflection of the fold mirror structure and the camera base, less than 0.1 arcsec/hr, should cause less than 0.01 pixel/hr image shifts based on Table 1.

If the entrance window is removed from the Binospec model, the fold mirror structure will experience $\pm 0.25^\circ$ C temperature variations and 0.80 arcsec/hr deflection rates. The side fold mirrors would then cause $0.80/\sim 20=0.04$ pixel/hr image shifts on the CCD. The deflection rate of the camera base doubles for the no-entrance-window model, but the image shifts remain below 0.01 pixel/hr.

TABLE 4
CAMERA BASE and FOLD MIRROR STRUCTURE
Spherical Bending Approximation — Axial Temperature Gradients

Case	ΔT ($^\circ$ C)	$\Delta T/dt$ ($^\circ$ C/hr)	θ_{worst} (arcsec)	$d\theta/dt$ (arcsec/hr)	z_{worst} (mil)	dz/dt (mil/hr)
Camera base	± 0.20	0.01	1.2	0.08	0.02	0.002
Fold mirror structure	± 0.05	0.004	0.4	0.03	0.01	0.001

6. FUTURE WORK

In November 1998 Henry Bergner completed a structural analysis of Binospec, one aspect of which was studying the effects of 10° F linear temperature gradients across the spectrograph. (Henry plotted the results of this in the "Binospec Thermal Gradient Analysis" memo, instrument database document #185.) Unfortunately the single-direction gradients are not very realistic. Our thermal models also show that a 10° F gradient is quite extreme for an insulated Binospec.

The next step is to incorporate the temperature distribution of our thermal model into Henry's finite element model. Henry can easily assign temperatures to finite element model nodes; the complicated aspect is to match the geometry of the nodes in my thermal model to his finite element model. To properly assign temperatures, I will mark up a node map (see Figure 5). I also recommend that I sit down with Henry when he assigns temperatures to his finite element model. The results of this next step will tell us how the Binospec structure deforms under typical temperature gradients.

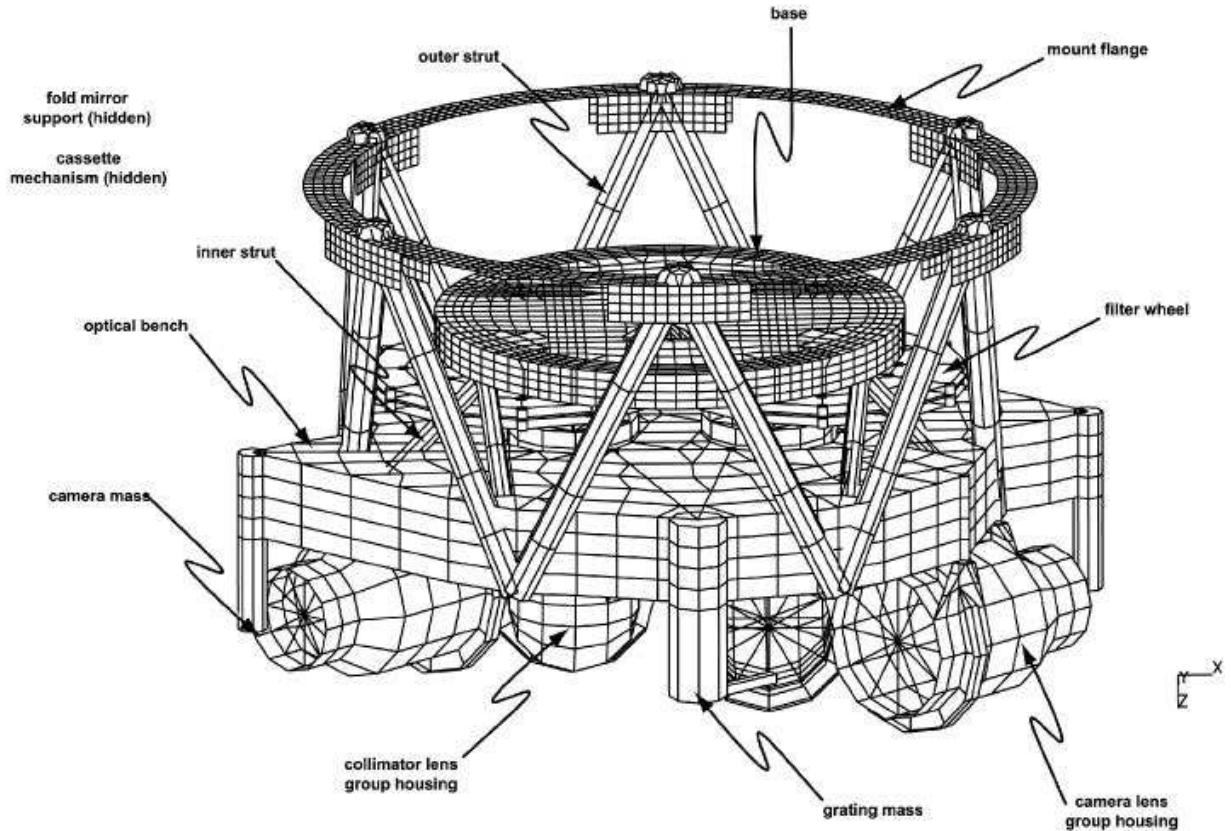


Fig. 5.— Henry Bergner's finite element model of Binospec.